TABLE 1 Proliferation of the MGF-dependent mast cell line MC-6 on established cell lines and transfected CV-1 cells

Cell line	^{3}H-thymidine incorporation (c.p.m.)
STO	6,728 ± 2,413*
NIH-3T3	9,849 ± 3,839†
CV-1	2,064 ± 138
CV-1 WT MGF	7,552 ± 575†
CV-1 Sl^d MGF	13,244 ± 1,917†
CV-1 + carrier	2,365 ± 492

Proliferation assays were essentially carried out as previously described[14]. Briefly, 20,000 feeder cells were plated into microtitre wells and irradiated with 5,000 rads to induce quiesence. After 24 h, 10,000 MC-6 cells were added to each well and after a further 24 h the cultures were pulsed for 4–5 h with 1 μCi [^{3}H]thymidine. Wells were collected on fibreglass filters with an automated collector and incorporated [^{3}H]thymidine counted by liquid scintillation spectrometry. This experiment was repeated four times with six replicates per treatment.

* $P \leq 0.05$ versus CV-1 cells or CV-1 + carrier.

† $P \leq 0.001$ versus CV-1 cells or CV-1 + carrier.

the total MGF produced by CV-1-Sl^d (assayed by mast cell proliferation) was higher than that of CV-1-Wt (Table 1). We also compared PGC survival on Sl/Sl^d (BM-Sl^d) and congenic wild-type (BM-Wt) bone marrow-derived stromal cell lines. BM-Sl^d supported PGC survival to 40% of BM-Wt after 1 day, but did not support subsequent PGC survival (Fig. 2*c*). When recombinant MGF (rMGF) was added to PGCs cultured on BM-Sl^d, PGC survival of over one day improved to 70% of BM-Wt, but subsequent PGC survival was unaffected (Fig. 2*c*). When rMGF was added to PGCs cultured on NIH-3T3 or STO cells, PGC survival was not enhanced (Fig. 2*b* and data not shown). Presumably, in the culture conditions used in this study, the amount of MGF produced by NIH-3T3 and STO cells is sufficiently high to support maximal PGC survival in the absence of added rMGF (see Fig. 1*b* and Table 1). Soluble MGF, such as that produced by Sl/Sl^d cells, is able to support only limited PGC survival and is unable to support long-term survival seen when PGC are cultured on wild-type cells producing both transmembrane and soluble MGF. In a similar study, Godin *et al.*[7] report that soluble factor is able to enhance initial survival (>48 h) but does not promote long-term survival of PGC cultured in the absence of STO cells.

The reduced ability of soluble MGF to support long-term survival may reflect a requirement for a localized, high concentration of MGF, for a particular conformation of MGF, for a role of MGF in promoting cell adhesion, or for an extended ligand-receptor interaction precluded by internalizable, soluble MGF. That transmembrane MGF is more effective in supporting PGC survival could provide (1) a mechanism both for the haptotactic guidance of PGCs to the gonad anlagen as well as for strict regulation of PGC proliferation and differentiation in the embryo and (2) a possible explanation for the sterility found in Sl/Sl^d mice. The viability, but sterility and lack of pigment, of Sl/Sl^d mice suggests that the haemopoietic lineages can be maintained to some extent by soluble factor, whereas PGCs and melanoblasts cannot. The activity of soluble factor on mast cells and primitive haemopoietic progenitors *in vitro*[14–16] and on mast cells *in vivo*[9] is consistent with this idea.

Binding of tyrosine kinase receptors, such as c-*kit*, by their cognate ligands usually leads to activation of the kinase domain and transduction of signals that lead to cellular proliferation[17–19]. The MGF/c-*kit* complex mediates a proliferation response in mast cells[14,15,20] and, in combination with other factors, proliferation of primitive haemopoietic progenitors[11,15,16,20,21]. The data presented here and by Godin *et al.*[7] provide the first evidence of growth factor action on mouse PGCs and suggest a role for MGF in mediating a PGC survival signal rather than a proliferation signal. □

Received 2 May; accepted 5 July 1991.

1. Orr, U. A. *et al. Development* **109,** 911–923 (1990).
2. Keshet, E. *et al. EMBO J.* (in the press).
3. Matsui, Y., Zsebo, K. M. & Hogan, B. L. *Nature* **347,** 667–669 (1990).
4. Donovan, P. J., Stott, D., Cairns, L. A., Heasman, J. & Wylie, C. C. *Cell* **44,** 831–838 (1986).
5. Godin, I., Wylie, C. & Heasman, J. *Development* **108,** 357–363 (1990).
6. Cairns, L. thesis, Univ. Lond. (1987).
7. Godin, I. *et al. Nature* **352,** 807–809 (1991).
8. Copeland, N. G. *et al. Cell* **63,** 175–183 (1990).
9. Zsebo, K. M. *et al. Cell* **63,** 213–224 (1990).
10. Huang, E. *et al. Cell* **63,** 225–233 (1990).
11. Flanagan, J. G., Chan, D. C. & Leder, P. *Cell* **64,** 1025–1035 (1991).
12. Brannan, C. I. *et al. Proc. natn. Acad. Sci. U.S.A.* **88,** 4671–4674 (1991).
13. McCoshen, J. A. & McCallion, D. J. *Experientia* **31,** 589–590 (1975).
14. Williams, D. E. *et al. Cell* **63,** 167–174 (1990).
15. Anderson, D. M. *et al. Cell* **63,** 235–243 (1990).
16. Zsebo, K. M. *et al. Cell* **63,** 195–201 (1990).
17. Hanks, S. K., Quinn, A. M. & Hunter, T. *Science* **241,** 42–52 (1988).
18. Pawson, T. & Bernstein, A. *Trends Genet.* **6,** 350–356 (1990).
19. Yarden, Y. & Ullrich, A. *A. Rev. Biochem.* **57,** 443–478 (1988).
20. Nocka, K., Buck, J., Levi, E. & Besmer, P. *EMBO J.* **9,** 3287–3294 (1990).
21. Martin, F. H. *et al. Cell* **63,** 203–211 (1990).
22. Chomczynski, P. & Sacchi, N. *Analyt. Biochem.* **162,** 156–159 (1987).
23. Church, G. M. & Gilbert, W. *Proc. natn. Acad. Sci. U.S.A.* **81,** 1991–1995 (1984).
24. Dugaiczyk, A. *et al. Biochemistry* **22,** 1605–1613 (1983).
25. Graham, F. L. & Eb, A.v.d. *Virology* **52,** 456–467 (1973).
26. Boswell, H. S., Albrecht, P. R., Shupe, R. E., Williams, D. E. & Burgess, J. *Expl Hemato.* **15,** 46–53 (1987).

ACKNOWLEDGEMENTS. We thank E. Jannini for his support and encouragement, K. Heston, J. R. Keller and G. Smith for practical help, E. Jannini, M. A. Bedell and L. Cheng for critically reading the manuscript and with N. G. Copeland, M. De Felici, N. A. Jenkins, J. R. Keller and L. F. Parada, for many helpful discussions. This work was supported in part by the National Cancer Instiute, DHHS, under contract with ABL.

Carboxy-terminal truncation activates *glp-1* protein to specify vulval fates in *Caenorhabditis elegans*

Susan E. Mango*, Eleanor M. Maine† & Judith Kimble*‡

* Laboratory of Molecular Biology and Department of Biochemistry, University of Wisconsin–Madison, 1525 Linden Drive, Madison, Wisconsin, 53706, USA

† Department of Biology, Syracuse University, Syracuse, New York 13214, USA

THE *glp-1* and *lin-12* genes encode homologous transmembrane proteins[1,2] that may act as receptors for cell interactions during development[3,4]. The *glp-1* product is required for induction of germ-line proliferation and for embryogenesis[3,5]. By contrast, *lin-12* mediates somatic cell interactions, including those between the precursor cells that form the vulval hypodermis (VPCs)[6]. Here we analyse an unusual allele of *glp-1*, *glp-1(q35)*, which displays a semidominant multivulva phenotype (Muv), as well as the typical recessive, loss-of-function Glp phenotypes (sterility and embryonic lethality)[3]. We find that the effects of *glp-1(q35)* on VPC development mimic those of dominant *lin-12* mutations, even in the absence of *lin-12* activity. The *glp-1(q35)* gene bears a nonsense mutation predicted to eliminate the 122 C-terminal amino acids, including a ProGluSerThr (PEST) sequence thought to destabilize proteins. We suggest that the carboxy terminus bears a negative regulatory domain which normally inactivates *glp-1* in the VPCs. We propose that inappropriate *glp-1(q35)* activity can substitute for *lin-12* to determine vulval fate, perhaps by driving the VPCs to proliferate.

During wild-type development, three VPCs (P5.p, P6.p, P7.p) generate 22 descendants that form the vulval hypodermis (Figs 1 and 2*a*). Several genes are known that, when mutant, interfere with this process (reviewed in ref. 7). One of these is *lin-12*: animals with elevated *lin-12* activity *(lin-12(d))* are Muv because all six VPCs adopt the VH2 fate[6]. The *glp-1* and *lin-12* genes

‡ To whom correspondence should be addressed.

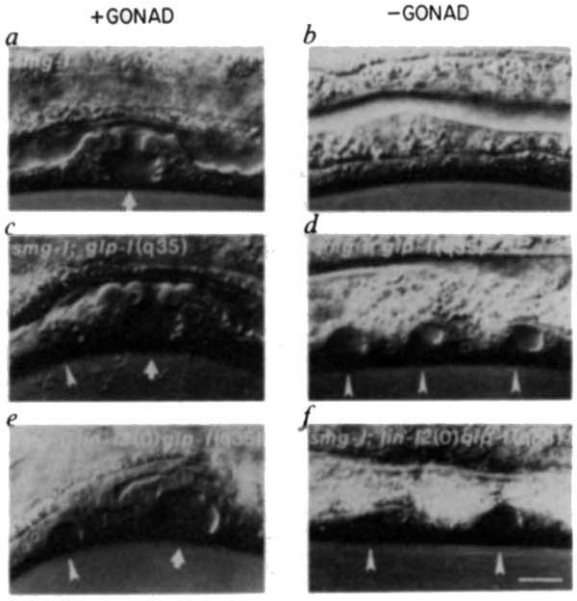

FIG. 1 Vulval phenotypes. Nomarski differential interference contrast (DIC) photomicrographs of fourth larval stage hermaphrodites. *a, c, e,* Intact animals that retain their gonad (+GONAD); *b, d, f,* animals that have had their gonad destroyed in early L1 (−GONAD). *a* and *b, smg-1; c* and *d, smg-1; glp-1(q35); e* and *f, smg-1; lin-12(0)glp-1(q35).* An arrow indicates the normal, AC-dependent vulval invagination; arrowheads indicate pseudovulval invaginations. Animals in *c, d, e* and *f* had additional pseudovulvae not shown in the figure. Scale bar ~10 μm.

METHODS. Alleles used were the loss-of-function allele *smg-1(r861) I* (ref. 10), the putative null allele *lin-12(n941) II* (ref. 6) and *glp-1(q35) III. smg-1;glp-1(q35) III* animals were maintained as a homozygous stock; *smg-1;lin-12(0)glp-1(q35)* animals from *smg-1;lin-12(0)glp-1(q35)/dpy-19(e1259)unc-69(e587)* mothers were identified by fate transformations typical of *lin-12(0),* such as an extra AC, or posterior ventral coelomocytes[6]. Nomarski DIC microscopy was performed as described[18]. Animals were maintained by standard laboratory techniques[19] at 20 °C (operated animals) and 23 °C (all others). To destroy the gonad, the somatic gonadal precursor cells Z1 and Z4 were killed during the first larval stage of hermaphrodites that had been anesthetized in 20 mM sodium azide/1 ×M9. Laser microsurgery was performed as described[20] using a Zeiss axioskop microscope, VSL-337 nitrogen laser, and DLM-110 dye laser module. Animals were examined in the third larval stage to ensure that the gonad was absent, and that there was no other structural damage.

a

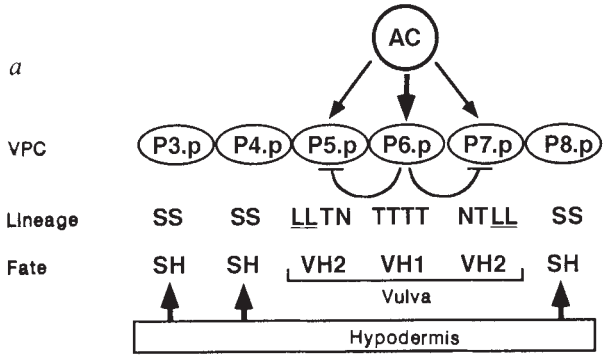

b

Expt	Geno type	Anchor cell	P3.p	P4.p	P5.p	P6.p	P7.p	P8.p
1	N2	+	SS	SS	LLTN	TTTT	NTLL	SS
2	*smg-1*	·	S	S	S	S	SS	S
3	*lin-12(d+)*	·	LLSL	LLLT	LLTN	LLTT	NTLL	LLLL
4			LLLL	LLLL	LLTT	NTLL	LQLL	SS
5	*lin-12(d d)*	·	SS	SS	LLLN	LLLL	NTLL	LLLL
6	*smg-1;*	+	LLLT	LLLL	LLTN	TTTT	NTLL	LLLL
7	*glp-1(q35)*		SS	SSSS	LLTN	TTTT	NTLL	LLNN
8			LNLT	LLLL	LLTN	TTTT	NTLL	SS
9			SS S	SS	LLTN	TTTT	NTLL	SS
10			LLLT	LLLL	LLTN	TTTT	NTLL	LLLN
11			SSLL	SSLL	LLTN	TTTT	NTLL	LLTL
12			SSLL	LLTN	TTTT*	NTLL	LLLL	SS
13	*smg-1;*	·	S LL	SS	SNLL	LLNN	LLLL	SS
14	*glp-1(q35)*		S	S	SS	LLLL	LLLN	LLLL
15			SS	SS	LLNT	LLLT	LLLT	LLLL
16			S NL	SS	SNLL	LLLL	SS	LL S
17			SS	LL S	LTLL	LLLT	LLLN	LL S
18	*smg-1;*	+	SLLL	LLLO	LLTT	TTTT	TTTT	NTLL
19	*lin-12(0)*		SS	S SS	NNTL	TTTT	NTLL	NLLL
20	*glp-1(q35)*		LLLL	LLLL	LLTN	TTTT	TTLL	SS
21			SS S	LLLL	LLTT	TTTT	NTLL	LLLL
22			SS S	SS	LLTN	TTTT	TTLL	LL S
23			LLLL	LLLL	LLTD	TTTT	NTLL	LLLL
24	*smg-1;*	·	LLLL	LLLT	LLTL	LLLL	LLLL	S OL
25	*lin-12(0)*		SS	SSLT	LLLL	LLLL	LLLL	LLLT
26	*glp-1(q35)*		LLLL	SS S	LLLL	LLLL	LLTN	LLTN†

FIG. 2 *a,* Model for wild-type vulval development; see ref. 7 for review. Three (P5.p, P6.p, and P7.p) of six vulval precursor cells (VPCs) located in the ventral hypodermis divide three times and form the vulval hypodermis (VH1 (or 1°) and VH2 (or 2°) fates)[18]. The remaining three cells (P3.p, P4.p, and P8.p) divide once and fuse with the hypodermal syncytium (SH (or 3°) fate)[18]. Each VPC has the potential to adopt the VH1, VH2 or SH fate[12,20,22]. In wild-type, however, the fate of each is invariant[18]. VH1 and VH2 fates are induced by the anchor cell (AC), a cell of the somatic gonad[12], whereas SH fate is promoted by a signal from the hypodermis (arrows)[21]. Although inductive signals are diagrammed as emanating directly from the AC and hypodermis, these signals may be indirect. The choice between VH1 and VH2 depends on the proximity of a VPC to the AC, and on a signal from the VH1 to the VH2 cell (bar)[22,23]. VH1 and VH2 fates are distinguished by the axis of the third division and the adherence of the progeny cells to the ventral cuticle[22]. Axes are either transverse (T), or longitudinal (L); no third division is designated as N. Cell divisions that generate adherent daughters are underlined; if daughters are nonadherent, the division axis is not underlined. Cells that fuse with the syncytial hypodermis are denoted by an S. The VH1 fate is characterized by four nonadherent divisions (normally TTTT), whereas the VH2 fate is characterized by two adherent divisions and 1–2 non-adherent divisions (usually NTLL or LLTN). *b,* Vulval fates in *glp-1(q35)* and *lin-12* mutants. The VPC lineages of the following animals were obtained: (1) wild-type (N2 animals with a gonad (*smg-1* animals behalve like N2 (ref. 10); (2) *smg-1* animals in which the gonadal precursors (and hence the AC) were destroyed by laser microsurgery; (3, 4) *lin-12(d)/+* and (5) *lin-12(d)* animals that lack an AC owing to cellular transformation[6]; (6–12) *smg-1;glp(q35)* animals with a gonad; (13–17) *smg-1;glp-1(q35)* animals in which the gonadal precursors were destroyed by laser microsurgery; (18–23) *smg-1;lin-12(0)glp-1(q35)* animals with a gonad; (24–26) *smg-1;lin-12(0)glp-1(q35)* animals in which the gonadal precursors were destroyed. Division axes are as described in *a.* In addition, oblique (O) divisions were occasionally seen. Cells that divided, but in which the plane of division was not observed, are marked as D. Each line represents an individual VPC lineage. Asterisk, the AC was centered over P5.p; dagger, P9.p followed a vulval lineage: LTLL.

METHODS. Alleles were the same as those listed in the legend to Fig. 1, as well as the dominant gain-of-function allele *lin-12(n952) III*[6]; *lin-12(d)* and *lin-12(d)/dpy-19lin-12(+)unc-69* animals were distinguished by progeny testing. Lineages were performed as described in the legend to Fig. 1.

encode similar proteins[1,2]. Furthermore, *lin-12* and *glp-1* are redundant during embryogenesis[8], and may be able to respond to the same signal from the gonadal anchor cell (AC)[9]. These observations raise the possibility that *glp-1(q35)* is Muv because it is mimicking *lin-12(d)*, so we have compared the effects of *glp-1(q35)* and *lin-12(d)* on vulval development.

Several observations indicate that the *glp-1(q35)* Muv phenotype results from increased or novel *glp-1* activity. First, this phenotype is dominant, whereas all *glp-1* loss-of-function mutations are recessive (Fig. 3*a* and *b*; ref. 3). Second, this class of mutation is rare (one GlpMuv per 10^4 haploid genomes; ref. 3, and our unpublished results). Third, *glp-1(q35)* homozygotes are more Muv than *glp-1(q35)/glp-1(0)* or *glp-1(q35)/+* heterozygotes (Figure 3*a*). Fourth, the informational suppressor, *smg-1* (ref. 10), suppresses the *glp-1(q35)* loss-of-function Glp phenotypes, but enhances its Muv phenotype (Fig. 3*b*). Certain mutants are rescued by *smg* mutations, apparently by increasing the abundance of aberrant RNAs (R. Pulak and P. Anderson, personal communication). By analogy, *smg-1* is predicted to increase the amount of *glp-1(q35)* RNA, and consequently protein, thereby suppressing the loss-of-function phenotypes and enhancing the gain-of-function phenotype.

To investigate whether the *glp-1(q35)* fate transformations are similar to those of *lin-12(d)*, we examined VPC development in *smg-1;glp-1(q35)* double mutants (Figs 1*c* and 2*b*). The double mutant was used to enhance the Muv phenotype. Whereas VPC fates are not altered in *smg-1* mutants[10], in *smg-1;glp-1(q35)* homozygotes, P3.p, P4.p and P8.p often follow a VH2-like fate rather than an SH fate (for example, see Fig. 2*b*, rows 6 and 10). Although other P(3,4,8).p lineages are harder to characterize, they are never VH1-like. These fate transformations are reminiscent of weak *lin-12(d)* alleles (Fig. 2*b*, rows 3–5).

In addition to the ectopic pseudovulvae made by P(3,4,8).p, a normal vulva is always formed in *smg-1;glp-1(q35)* animals, indicating that the VPCs are still responsive to the anchor cell signal. This is especially apparent when the AC is mispositioned, and the vulva is shifted accordingly (Fig. 2*b*, row 12). Similarly, when an AC is present in *lin-12(d)* mutants, the VPCs respond to it[11].

We next asked whether the *glp-1(q35)* Muv phenotype, like that of *lin-12(d)*, is independent of the AC. To address this question we destroyed the gonadal precursor cells during the first larval stage, before the AC is born. Although no vulva develops in wild type[12] and *smg-1* animals lacking an AC (Figs 1*b* and 2*b*, row 2), pseudovulvae are still made in *smg-1;glp-1(q35)* animals without an AC (Figs 1*d* and 2*b*, rows 13–17). Thus, *glp-1(q35)* does not act in the gonad to promote pseudovulvae formation, nor does *glp-1(q35)* require a signal from an AC or VH1 cell, as these cell types are not formed in ablated animals. Interestingly, P(5–7).p are more likely to follow a vulval fate in ablated animals than P(3,4,8).p (Fig. 2*b*, rows 13–17). This bias may reflect a difference between the cells themselves (for example, wild-type P(5–7).p versus P(3,4,8).p), or their environments. Alternatively, *glp-1(q35)* may affect

	Number of pseudovulvae* 0	1	2	3	4	%Muv†	%Glp‡	% Survival of progeny§
a Dosage								
glp-1(+)	60	0	0	0	0	0%	0% (n=60)	98% (n=284)
glp-1(q35)	11	39	8	3	2	83%	94% (n=70)	0% (n=9)
glp-1(q35)/+	47	16	2	0	0	28%	0% (n=65)	98% (n=214)
glp-1(q35)/glp-1(0)	51	14	2	1	1	26%	100% (n=69)	NA
b Effect of *smg-1*								
smg-1;glp-1(+)	60	0	0	0	0	0%	0% (n=60)	98% (n=170)
smg-1;glp-1(q35)	4	13	20	19	3	93%	3% (n=59)	25% (n=175)
smg-1;glp-1(q35)/+	27	22	11	0	0	55%	0% (n=60)	99% (n=190)

FIG. 3 Characterization of *glp-1(q35)* Muv and Glp phenotypes. *a*, Dosage studies with *glp-1(q35);glp-1(q35)* and *glp-1(q35)/dpy-19glp-1(+)unc-69* animals were obtained from *glp-1(q35)/dpy-19glp-1(+)unc-69* mothers at 23 °C. Genotypes were identified by progeny testing; *glp-1(q35)/glp-1(0)* animals were obtained by mating *glp-1(q35)/dpy-19glp-1(+)unc69* hermaphrodites that had no more self-sperm with *glp-1(q46)/dpy-19glp-1(+)unc-69;him-5(e1490)* males. *glp-1(q46)* is null by genetic[3] and molecular criteria: it carries a nonsense mutation in the extracellular domain (V. Kodoyianni *et al.*, manuscript in preparation). The success of each mating was assayed by comparing the number of XX and XO progeny, and the number of *glp-1(q35)/+* to *glp-1(q46)/+* F1 hermaphrodites. *glp-1(q35)/(q46)* animals were identified by their Glp phenotype. *b*, *smg-1* enhances the Muv phenotype and suppresses the Glp phenotypes of *glp-1(q35)*. *smg-1;glp-1(q35)* and *smg-1;glp-1(q35)/dpy-19glp-1(+)unc-69* hermaphrodites from *smg*-1;*glp*-1(*q*35)/*dpy*-19*glp*-1(+)*unc*-69 mothers were identified by progeny testing at 23 °C.

* The number of pseudovulvae in young adult or fourth larval stage (L4) animals was determined by Nomarski DIC optics: We used these optics so that the effects of *smg-1* on vulval morphogenesis[10] did not alter our assessment of the presence or absence of pseudovulvae.

† The percentage of Muv animals was calculated using the data from the preceding columns.

‡ Single L4 animals were picked to individual plates and allowed to lay eggs overnight. Animals without embryos were scored as Glp.

§ L4 hermaphrodites were picked to individual plates, and allowed to lay eggs. Animals were moved daily, 24 hours after an animal was removed, its progeny were scored as unhatched eggs, L1 larval lethals or viable.

NA, not applicable; 0, null; +, wild type.

c, *glp-1(q35)* activity is required at the time of VPC determination. The *glp-1(q35)* mutation is temperature-sensitive: animals raised at 25 °C are often Muv and fertile, whereas those grown at 12° are generally non-Muv and Glp. For the downshift, *glp-1(q35)/dpy-19glp-1(+)unc-69* hermaphrodites were allowed to lay eggs for short periods of time (~1 h) at 25 °C. Animals were then removed, and the eggs allowed to develop at 25 °C until the stage indicated. Larvae were staged by Nomarski differential interference contrast (DIC) optics using standard criteria[18]. Larvae of the appropriate age were transferred to 12 °C plates, allowed to develop, and scored as adults. Homozygous *glp-1(q35)* animals were identified by the presence of meiotic germ cells in the distal arm of the gonad, and examined for pseudovulvae and eggs by Nomarski DIC microscopy as adults. Equivalent procedures were used for the upshift (12 °C to 25 °C). L1–L4, First through to the fourth larval stagres; 0÷, 1x÷ and 2x÷ indicate the number of Pn.p cell divisions;

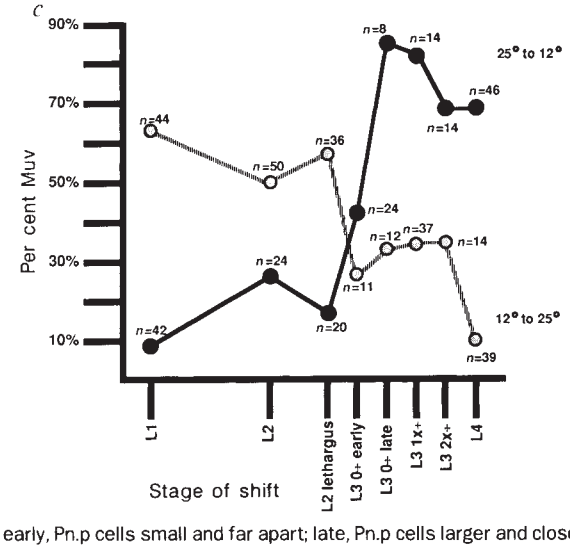

early, Pn.p cells small and far apart; late, Pn.p cells larger and close together; filled circles, worms were shifted from 25 °C to 12 °C; open circles, worms were shifted from 12 °C to 25 °C; n is the number of *glp-1(q35)* animals assayed per timepoint.

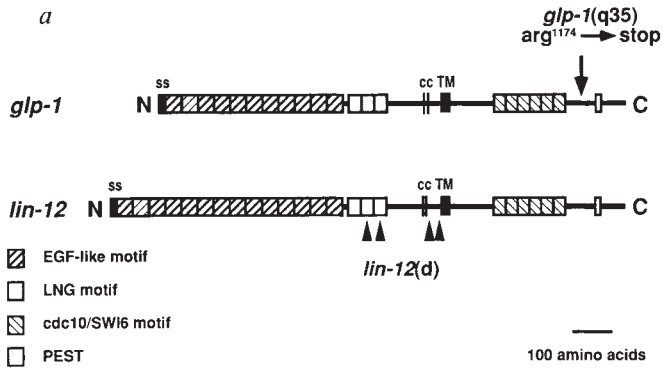

FIG. 4 *glp-1(q35)* is a nonsense mutation that removes the carboxy-terminal portion of the protein. *a*, The predicted proteins of *lin-12* and *glp-1* are shown for comparison[1,2,24,25]. Both are transmembrane proteins with a signal sequence (ss) and membrane-spanning domain (TM); both carry three repeated motifs, one similar to epidermal growth factor (EGF-like), one found in *lin-12, Notch* and *glp-1* (LNG), and a third found in cell-cycle regulators and ankyrin (cdc10/SW16). Also shown is the position of two cysteines conserved in *glp-1,lin-12* and *Notch*((CC) and a sequence proposed to act as a protein degradation signal (PEST). *glp-1* and *lin-12* are very closely linked on chromosome III (<0.02 centimorgans or ~18 kilobases[1-3]). In *glp-1(q35),* a CGA codon (encoding Arg 1,174) has been changed to a TGA stop codon (arrow). The approximate locations of the *lin-12(d)* mutations, all of which are missense[26], are indicated by arrowheads. *b*, The 122 amino acids predicted to be lost from the cytoplasmic domain of the *glp-1(q35)* protein are shown aligned with the corresponding region of *lin-12*. A strong PEST sequence encoded by both genes is underlined. Identities are shown by vertical lines, conservative changes by dots. The alignment is from ref. 2.

b

```
glp-1:  QQIVKSGHGA  KSGRQTVKNI  KRAGSRKTPT  SAASSRETNH  LTPPPSDGSF  SSPSP-HYYP  TTTSTPNRME
lin-12: LHI-QHTHQP  QPSRKVTRAP  KKQTSRSKKE  SASNSRDSTH  LTPPPSDGST  STPSPQHFMN  TTHTTPTSLN

glp-1:  -TSPEYMFNH  EMAPPVNA--  -------MWY  T-TPPPYQDP  NYRHVPPNTA  FQNAEQMNGS  FYC
lin-12: YLSPEYQTEA  GSSEAFQPQC  GAFGNGEMWY  TRASTSYTQM  QNEPMTRYSE  PAHYF
```

METHODS. The *glp-1(q35)* mutation was identified using a modification of the mismatch detection method[27]. The *glp-1(q35)* allele was isolated from a recombinant DNA library constructed from *glp-1(q35)/glp-1(q35);qDp3* hermaphrodites [*qDp3* is *glp-1(+)*]. Genomic DNA was cleaved with *Xho*I ligated to EMBL3 lambda phage vector cut with *Sal*I. The *glp-1(q35)* recombinants isolated this way contained ~2 kilobase pairs of 5′ flanking sequences. The protocol described in ref. 27 was modified as follows: (1) recombinant DNAs were restricted to produce fragments of 100–800 base pairs in the region to be probed; (2) after hybridization, duplexes were digested with 0.4 $\mu g\ \mu l^{-1}$ of RNase A (Sigma). We used a series of five probes (described in V. Kodoyianni *et al.*, manuscript in preparation) covering the entire gene and flanking sequences. Both *glp-1(+)* and *glp-1(q35)* clones were isolated, and the two classes of recombinants were distinguished by mismatch detection. The carboxy terminal PEST sequence was identified using the IBM PC Gene program of Intelligenetics, using the algorithm of Rogers *et al.*[14] The PEST sequence of *glp-1* scored 10.8 (>5 considered 'good').

individual VPCs differently. This same phenomenon is observed in *lin-12(d)* mutants (Fig. 2*b*, rows 3–5; ref. 13, and data not shown).

The *glp-1(q35)* mutation is temperature-sensitive, which allowed us to determine when *glp-1(q35)* activity is needed for the Muv phenotype. Temperature-shift experiments show that *glp-1(q35)* acts before the first P(3–8).p division (Fig. 3*c*), at the time of VPC determination[12]. At this time most *glp-1(+)* messenger RNA is found in the soma[1]; *lin-12(d)* activity is also required at this stage to determine VH2 fate[6].

The parallels between the effects of *glp-1(q35)* and *lin-12(d)* on vulval fate are striking. Both promote the VH2 fate among the VPCs, independently of an AC or VH1 cell; both result from a gain of gene function acting at the time of VPC determination. These similarities suggested that *glp-1(q35)* might affect VPC development by activating *lin-12* itself. To test this hypothesis we examined whether functional *lin-12* was necessary for the *glp-1(q35)* Muv phenotype. We found that *smg-1;lin-12(0)glp-1(q35)* animals still form pseudovulvae, either with a gonad or without one (Fig. 1*e*,*f* and 2*b*, rows 18–26). Thus, *lin-12* activity is not required for the *glp-1(q35)* Muv phenotype. Moreover, this is the first report of a VPC able to adopt a VH2 fate in the absence of functional *lin-12*. We therefore propose that *glp-1(q35)* can substitute for *lin-12* to direct development of the vulval hypodermis.

Although the effect of *glp-1(q35)* on the VPCs mimics that of *lin-12(d)*, other fate transformations typical of *lin-12(d)* do not appear to be affected by *glp-1(q35)* (data not shown). We do not know whether this difference reflects a dissimilarity in gene expression or protein function. For example, *glp-1(q35)* may not be expressed in the same tissues as *lin-12(d)*, and therefore could not alter these other cell fate decisions.

The *glp-1(q35)* mutation is associated with a C to T base transition that changes the triplet encoding arginine at position 1174 to a stop codon, truncating the predicted *glp-1* peptide by 122 amino acids (Fig. 4). Both the recessive Glp and dominant Muv phenotypes are likely to stem from this single lesion as both are affected by *smg-1* and both are temperature-sensitive. Furthermore, because *lin-12* activity is not required, the Muv phenotype associated with *glp-1(q35)* cannot be explained by a closely linked *lin-12(d)* mutation.

The region removed by the *glp-1(q35)* mutation is unlike that of *lin-12*, except for a short PEST sequence (Fig. 4*b*). Such sequences are thought to be degradation signals[14]. Supporting this hypothesis, mutations that alter a PEST-like sequence in the *ftz* gene stabilize the protein and cause dominant, gain-of-function phenotypes[15]. Similarly, the *glp-1(q35)* Muv phenotype may result from an increase of *glp-1* protein. In addition, the carboxy-terminal truncation may either destroy a more specific negative regulatory domain, thereby derepressing normal *glp-1* activity, or alter the specificity such that the *glp-1(q35)* protein can interact with factors that the normal *glp-1* product cannot.

The *glp-1(q35)* mutation generates loss-of-function Glp phenotypes in addition to the gain-of-function Muv phenotype. This reduction in *glp-1* activity may reflect a less active protein, or a decreased amount of protein resulting from destabilized mRNA, an effect seen with other nonsense mutations (see for example, ref 16). Consistent with the latter hypothesis is the efficient suppression of the Glp phenotypes by *smg-1*. Because the *glp-1(q35)* truncated protein is functional in a *smg-1* background we propose that the carboxy-terminal 122 amino acids of the *glp-1* protein are not essential. Furthermore, we suggest that the distinct roles of *glp-1* and *lin-12* in development rely on gene-specific regulation rather than on unique functional domains.

As wild-type *glp-1* acts in the germ line to promote mitosis[3], we speculate that *glp-1(q35)* may act in the vulval hypodermis by promoting proliferation. Likewise, some cell fate decisions

that require *lin-12* are also proliferative[6]. Many mammalian growth factors (for example, colony-stimulating factor-1; ref. 17) promote both proliferation and differentiation. Perhaps these processes are similarly linked in *C. elegans*, and by driving proliferation, *glp-1(q35)* influences a VPCs subsequent fate. □

Received 11 June; accepted 17 July 1991.

1. Austin, J. & Kimble, J. *Cell* **58,** 565–571 (1989).
2. Yochem, J. & Greenwald, I. *Cell* **58,** 553–563 (1989).
3. Austin, J. & Kimble, J. *Cell* **51,** 589–599 (1987).
4. Seydoux, G. & Greenwald, I. *Cell* **57,** 1237–1245 (1989).
5. Priess, J. R., Schnabel, H. & Schnabel, R. *Cell* **51,** 610–611 (1987).
6. Greenwald, I. S., Sternberg, P. W. & Horvitz, H. R. *Cell* **34,** 435–444 (1983).
7. Horvitz, H. R. & Sternberg, P. W. *Nature* **351,** 535–541 (1991).
8. Lambie, E. J. & Kimble, J. *Development* **112,** 231–240 (1991).
9. Seydoux, G., Schedl, T. & Greenwald, I. *Cell* **51,** 939–951 (1990).
10. Hodgkin, J., Papp, A., Pulak, R., Ambros, V. & Anderson, P. *Genetics* **123,** 301–313 (1989).
11. Sternberg, P. W. & Horvitz, H. R. *Cell* **58,** 679–693 (1989).
12. Kimble, J. *Devl Biol.* **87,** 286–300 (1981).
13. Seydoux, G. thesis, Univ. Princeton (1991).
14. Rogers, S., Wells, R. & Rechsteiner, M. *Science* **234,** 364–368 (1986).
15. Kellerman, K. A., Mattson, D. M. & Duncan, I. *Genes Dev.* **4,** 1936–1950 (1990).
16. Losson, R. & Lacroute, F. *Proc. natn. Acad. Sci. U.S.A.* **76,** 5134–5137 (1979).
17. Stanley, E. R., Guilbert, L. J., Tushinski, R. J. & Bartelmez, S. H. *J. Cell Biochem.* **21,** 151–159 (1983).
18. Sulston, J. & Horvitz, H. R. *Devl Biol.* **56,** 110–156 (1977).
19. Brenner, S. *Genetics* **77,** 71–94 (1974).
20. Sulston, J. E. & White, J. G. *Devl Biol.* **78,** 577–597 (1980).
21. Herman, R. K. & Hedgecock, E. M. *Nature* **348,** 169–171 (1990).
22. Sternberg, P. W. & Horvitz, H. R. *Cell* **44,** 761–772 (1986).
23. Sternberg, P. W. *Nature* **335,** 551–554 (1988).
24. Greenwald, I. *Cell* **43,** 583–590 (1985).
25. Yochem, J., Weston, K. & Greenwald, I. *Nature* **335,** 547–550 (1988).
26. Greenwald, I. & Seydoux, G. *Nature* **346,** 197–199 (1990).
27. Myers, R. M., Larin, Z. & Maniatis, T. *Science* **230,** 1242–1246 (1985).

ACKNOWLEDGEMENTS. We thank T. Schedl, I. Greenwald and P. Sternberg for critical comments on the manuscript, members of the laboratory, especially E. Lambie, for discussion, G. Beitel and H. Horvitz for *lin-12(n952)*, S. Crittenden for running the PEST algorithm, and P. Balandyk and L. Olds for technical assistance. Some strains used in this work were provided by the *Caenorhabditis* Genetics Center, which is funded by the NIH NCRR, S.E.M. is a Helen Hay Whitney Fellow. This work was supported by the N.I.H.

Human dystrophin expression in mdx mice after intramuscular injection of DNA constructs

Gyula Acsadi*†, George Dickson‡, Donald R. Love§, Agnes Jani*, Frank S. Walsh‡, Asitha Gurusinghe§, Jon A. Wolff*|| & Kay E. Davies§

* Departments of Pediatrics and Medical Genetics, Waisman Center, University of Wisconsin, Madison, Wisconsin 53706, USA
‡ Department of Experimental Pathology, UMDS, Guy's Hospital, London Bridge, London SE1 9RT, UK
§ Molecular Genetics Group, Institute of Molecular Medicine, John Radcliffe Hospital, Headington, Oxford OX3 9DU, UK

DUCHENNE'S muscular dystrophy (DMD), which affects one in 3,500 males, causes progressive myopathy of skeletal and cardiac muscles and premature death[1]. One approach to treatment would be to introduce the normal dystrophin gene into diseased muscle cells. When pure plasmid DNA is injected into rodent skeletal[2] or cardiac muscle[3–5], the cells express reporter genes. We now show that a 12-kilobase full-length human dystrophin complementary DNA gene and a 6.3-kilobase Becker-like gene[6] can be expressed in cultured cells and *in vivo*. When the human dystrophin expression plasmids are injected intramuscularly into dystrophin-deficient mdx mice, the human dystrophin proteins are present in the cytoplasm and sarcolemma of ~1% of the myofibres. Myofibres expressing human dystrophin contain an increased proportion of peripheral nuclei. The results indicate that transfer of the dystrophin gene into the myofibres of DMD patients could be beneficial, but a larger number of genetically modified myofibres will be necessary for clinical efficacy.

A human full-length[7] or a Becker-like cDNA dystrophin sequence was inserted into expression vectors containing either the Rous sarcoma virus (RSV) or cytomegalovirus (CMV) promoters (Fig. 1). In cultured Cos cells transfected with constructs containing either the Becker-like sequence (pCMVDy-B) or the construct containing the full-length dystrophin sequence (pRSVDy), a dystrophin protein of relative molecular mass (M_r) 200,000 (200K) (Fig. 2*a*, lane 3) or 427K (Fig. 2*a*, lane 4), respectively, was detected on immunoblots. Some 30% of Cos

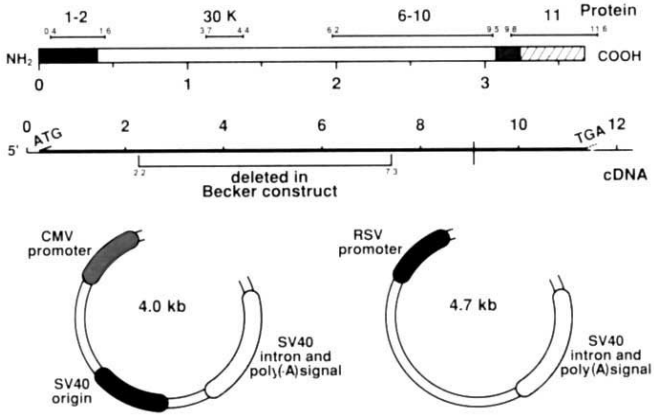

FIG. 1 Diagrammatic representation of the human dystrophin cDNAs, protein and related antibodies. The full-length dystrophin construct corresponds to a segment of cDNA of ~12 kb (112 bp to 12,101 bp; ref. 25) encoding the principal skeletal muscle isoform of human dystrophin[7]. The 6.3-kb Becker-like dystrophin construct was made in three parts. (1) PCR amplification across the exon 16/49 boundary: plasmid pCf56a and the 2.2-kb *Eco*RI insert of pCf27 (ref. 26) were amplified by PCR using oligonucleotides M13-forward (BRL) plus 5′-GAAAAGAGTACAGCACAGGAAACTGAAATA-GCAGTT-3′ (324J-LF) and 5′-CTGGCCGTTTTAAAAGCG-3′ (324J-F) plus 5′-AACTGCTATTTCAGTTTCCTGTGCTGTACTCTTTTC-3′ (324J-LR), respectively. Oligonucleotides 324J-LF and 324J-LR are complementary with the dystrophin exon 16/49 boundary at the mid-position in each oligonucleotide. Amplification by PCR consisted of 15 cycles of 94 °C for 1 min, 45 °C for 30 s and 72 °C for 1 min with each oligonucleotide present at 1 μM[27]. One-fiftieth of each PCR was pooled and amplified for 30 cycles using oligonucleotides M13-forward and 324J-F (5′ nucleotide at dystrophin position 2,015). The DNA product was subsequently digested with *Xba*I plus *Eco*RI and the 740-bp fragment introduced into double-digested pUC18 (Stratagene). A recombinant plasmid containing the correct PCR product (5′ and 3′ ends at dystrophin nucleotide positions 2,036 and 7,879) was determined by restriction enzyme digestion and sequencing of both DNA strands using the Sequenase Kit (USB). (2) 5′-end construction: the plasmid recombinant and pCf27 were digested with *Eco*RI then with *Bgl*II to give complete or partial digestion, respectively, at dystrophin nucleotide position 2,083. Fragments of ~690 bp (boundary PCR clone) and 1,971 bp (Cf27 from nucleotide position 112 to 2,083) were pooled, ligated in equimolar amounts and digested with *Eco*RI. the 2.7-kb fragment was isolated and ligated into the *Eco*RI site of pUC18. (3) 3′-end construction: the 4.3-kb *Eco*RI insert of pCf115 (ref. 26) was partially digested with *Hin*dII (at nucleotide position 11,512), and the 3.6-kb dystrophin fragment ligated into *Eco*RI plus *Sma*I-digested pUC18. This recombinant plasmid was digested with *Eco*RI (nucleotide position 7,876) plus *Sal*I (3′ end in multiple cloning site (MCS) of pUC18) and the dystrophin insert ligated with an equimolar amount of the 2.7-kb insert recovered from the recombinant, which had been digested to completion with *Sal*I (5′ end in MCS of pUC18) and partially with *Eco*RI (nucleotide position 7,875). The ligated DNAs were digested with *Sal*I and the 6.3-kb fragment ligated into the *Sal*I site of pUC18. The dystrophin cDNAs were inserted into the RSV promoter construct derived from pRSVLacZ (ref. 24) or the polylinker site of the pCDNAI plasmid (Invitrogen). pCDNAI contains a CMV promoter and the SV40 poly(A) addition signal, intron and origin of replication. The regions of dystrophin that were used to produce antibodies are represented by the bars above the protein[9–14]. The numbers at the beginning and end of the brackets indicate the corresponding dystrophin cDNA sequences.

† Present address: Department of Pediatrics, University Medical School of Pecs, H-7623, Hungary.
|| To whom correspondence should be addressed.